

# The observed covariance between ecosystem carbon exchange and atmospheric boundary layer dynamics at a site in northern Wisconsin

C. Yi,<sup>1,2</sup> K.J. Davis,<sup>1</sup> P.S. Bakwin,<sup>3</sup> A. S. Denning,<sup>4</sup> N. Zhang,<sup>4</sup> A. Desai,<sup>1</sup> J. C.-H. Lin,<sup>5</sup> C. Gerbig<sup>5</sup>

<sup>1</sup> Department of Meteorology, the Pennsylvania State University, University Park, PA 16802, USA.  
Chuixiang Yi (814-865-9617; [cxyi@essc.psu.edu](mailto:cxyi@essc.psu.edu))  
Kenneth J. Davis (814-863-8601; [davis@essc.psu.edu](mailto:davis@essc.psu.edu))  
Ankur Desai (814-865-9617; [adesai@essc.psu.edu](mailto:adesai@essc.psu.edu))

<sup>2</sup> MOE Key Laboratory of Environmental Change and Natural Disaster, IRS, Beijing Normal University, Beijing 100875, China.

<sup>3</sup> NOAA Climate Monitoring and Diagnostics Laboratory, 325 Broadway, Boulder, CO 80305, USA.  
Peter S. Bakwin (303-497-6773 [peter.bakwin@noaa.gov](mailto:peter.bakwin@noaa.gov))

<sup>4</sup> Department of Atmospheric Science, Colorado State University, Fort Collins, CO 80523-1371, USA  
A.Scott. Denning (970-491-6936 [denning@atmos.colostate.edu](mailto:denning@atmos.colostate.edu))  
N. Zhang (970-491-8526 [ni@dendrus.atmos.colostate.edu](mailto:ni@dendrus.atmos.colostate.edu))

<sup>5</sup> Department of Earth and Planetary Sciences, Harvard University, Cambridge, MA 02138, USA.  
Christoph Gerbig (617-495-9624 [chg@io.harvard.edu](mailto:chg@io.harvard.edu))  
John Ch.-H. Lin (617-495-5361 [johnlin@fas.harvard.edu](mailto:johnlin@fas.harvard.edu))

Correspondence: Chuixiang Yi  
Department of Meteorology  
The Pennsylvania State University  
416 Walker Building  
University Park, PA 16802  
Phone: (814) 865-9617  
Fax: (814) 865-3663  
Email: [cxyi@essc.psu.edu](mailto:cxyi@essc.psu.edu)

## **Abstract**

Ecosystem CO<sub>2</sub> exchange and atmosphere boundary layer (ABL) mixing are correlated diurnally and seasonally. Tracer transport models predict that these covariance signals produce a meridional gradient of annual mean CO<sub>2</sub> concentration in the marine boundary layer that is half as strong as the signal produced by fossil fuel emissions. This rectifier effect is simulated by most global tracer transport models. However, observations to constrain the strength of these covariance signals in nature are lacking. We investigate the covariance between ecosystem carbon dioxide exchange and ABL dynamics by comparing one widely cited transport model with observations in the middle of the North American continent. We measured CO<sub>2</sub> flux and mixing ratio using an eddy-covariance system from a 447-m tower in northern Wisconsin, mixed layer depths using a 915-MHz boundary layer profiling radar near the tower, and vertical CO<sub>2</sub> profiles from aircraft in the vicinity of the tower. We find (1) that simulated and observed net daily CO<sub>2</sub> fluxes are similar; (2) the simulated maximum ABL depths were too shallow throughout year; (3) the simulated seasonal variability of free troposphere CO<sub>2</sub> is 3 ppm less than the observations; and (4) the simulated seasonal covariance between CO<sub>2</sub> flux and mixing ratio is stronger than the observed covariance. The comparison between model and observations is limited by the questionable representativeness of a single observing site and a bias towards fair weather observing conditions.

## **1. Introduction**

The influence of terrestrial CO<sub>2</sub> exchange on the distribution of CO<sub>2</sub> in the atmosphere is modulated by the dynamics of the atmospheric boundary layer (ABL). On summer days, the depletion of CO<sub>2</sub> due to photosynthetic uptake is diluted by deep convective mixing, while at night,

CO<sub>2</sub> from respiration accumulates near the surface in a shallow, stable ABL. Outside of the tropics, a similar covariance occurs over seasonal scales. The covariance between terrestrial CO<sub>2</sub> exchange and vertical mixing influences the time-mean vertical partition of CO<sub>2</sub> between the ABL and free troposphere (FT) [Denning *et al.*, 1995].

Atmospheric inversion calculations infer the distribution of surface sources and sinks from distributions of CO<sub>2</sub> observed at a network of air sampling stations primarily located in the marine boundary layer (MBL) [Tans *et al.*, 1990]. Most tracer transport models [Denning *et al.*, 1996a,b; Law and Simmonds, 1996a; Law and Rayner, 1999; Bousquet *et al.*, 2000] used for these calculations predict elevated concentrations of CO<sub>2</sub> at MBL stations downwind of the temperate continents due to rectification of purely seasonal exchange with terrestrial biota (i.e., CO<sub>2</sub> exchange with a zero annual mean at each model grid cell). This enhances the simulated annual mean north-south CO<sub>2</sub> gradient and since observations show only a modest north-south gradient [Tans *et al.*, 1990; Conway *et al.*, 1994], this implies a larger compensating temperate sink in the inverse calculations. The strength of this rectifier effect on the simulated annual mean Arctic-to-Antarctic difference in the MBL varies from slightly negative to more than 2.5 ppm among different transport models [Law *et al.*, 1996b], and is one of the largest sources of uncertainty in estimates of continental-scale carbon fluxes [Gurney *et al.*, 2002, 2003]. The covariance between ecosystem CO<sub>2</sub> fluxes and the ABL dynamics drives the rectifier effect. However, observations to constrain the strength of the rectifier effect in nature are lacking. Continuous observations of atmosphere-ecosystem exchange of CO<sub>2</sub> (NEE) (e. g., FLUXNET, Baldocchi *et al.*, 2001) combined with long-term continuous measurements of ABL structure using boundary layer profiling radar [Ecklund *et al.*, 1988; Angevine *et al.*, 1998] can provide the data that is needed to assess the covariance.

In this study, a radar profiler and radiosonde system were deployed from 15 March to 3 November 1998, near a 447 m tall TV transmitter tower in northern Wisconsin. The tower was instrumented to continuously measure the turbulent flux of latent and sensible heat, and flux and mixing ratio profiles of CO<sub>2</sub>. The ML depths were derived from the signal-to-noise ratio (SNR) recorded by the radar profiler [Yi *et al.*, 2001], were verified against data from radiosondes. Measurements of CO<sub>2</sub> mixing ratio at 11, 30, 76, 122, 244, and 396 m above the ground allowed us to estimate stable ABL height at night, and give the CO<sub>2</sub> jump across the top of the nighttime stable ABL directly. The CO<sub>2</sub> jump across the top of ML during daytime was estimated from a jump model [Yi *et al.*, 2001; Tennekes, 1973] driven with the observed ML depth, CO<sub>2</sub> mixing ratios and eddy covariance flux data. During the morning when the ML top is below 400 m, the CO<sub>2</sub> jump across the top of the ML can be observed from measurements on the tower, thus providing a test for the jump model. The estimates of the CO<sub>2</sub> jump under deep mixing conditions are compared to aircraft measurements to test our ability to infer FT CO<sub>2</sub> mixing ratios from tower measurements.

## **2. Materials and Methods**

### **2.1 Site and Measurements**

The study site is located in Chequamegon National Forest in northern Wisconsin (45.95°N, 90.27°W; elevation 473 m). The region is in a heavily forested zone of low relief. The tower is a 447 m tall television transmitter surrounded by a grassy clearing of about 180 m radius. The site, instrumentation and flux calculation methodology have been described by Bakwin *et al.* [1998] and

*Berger et al.* [2001]. Three-axis sonic anemometers at 30, 122 and 396 m above ground are used to measure turbulent winds and virtual potential temperature. Air from these three levels is drawn down tubes to a trailer where three LI-COR 6262 analyzers are used to determine CO<sub>2</sub> and water vapor mixing ratio fluctuations at 5 Hz for eddy covariance flux measurements [*Berger et al.*, 2001]. High-precision, two-minute mean CO<sub>2</sub> mixing ratios are sampled at 11, 30, 76, 122, 244 and 396 m by two LI-COR 6251 analyzers [*Bakwin et al.*, 1998]. Measurements of the net ecosystem exchange (NEE) of CO<sub>2</sub> are described by *Davis et al.* [2003].

A National Center for Atmospheric Research (NCAR) Integrated Sounding System (ISS), which includes a clear-air wind-profiling radar, a Radio Acoustic Sounding System (RASS) and a balloon borne radiosonde system, was deployed about 8 km east of the tower from 15 March to 3 November, 1998. The profiler is a sensitive 915 MHz Doppler radar that is designed to respond to fluctuations of the refractive index in clear air [*Ecklund et al.*, 1988; *White et al.*, 1991; *Angevine et al.*, 1994]. The reflectivity measured by the profiler is related to the turbulence intensity, gradients of temperature and humidity, and particulates [*Ottersten*, 1969; *Wyngaard and LeMone*, 1980; *White et al.*, 1991]. The ML depth ( $z_i$ ) is derived from the SNR recorded by the profiler [*Yi et al.*, 2001]. The profiler can be used to measure  $z_i$  with a time resolution of 30 minutes or less, a height resolution of 60 to 100 m, a minimum height of 150 m, and a maximum height of 1500 to 3000 m depending on conditions [*Angevine et al.*, 1994]. ML depth cannot be estimated from the profiler SNR under unfavorable weather conditions such as rain, snow or heavy clouds. The profiler is very sensitive to large cloud droplets and raindrops resulting in a high, relatively featureless SNR over the depth of the precipitation shaft. Under these conditions, the boundary layer is often not clearly defined [*Stull*, 1988].

Mixed layers shallower than 400 m, which typically occur in morning, are also not well defined from the profiler SNR measurements. The CO<sub>2</sub> mixing ratio measurements from the tower were used to obtain  $z_i$  when it was below 400 m. The top of the mixed layer is defined as the depth above ground to which the CO<sub>2</sub> mixing ratio is constant with height, provided that the net radiation is positive (warming the Earth's surface) [Yi *et al.*, 2001].

The stable nocturnal ABL is typically very shallow, usually less than 200 m, and was estimated from the CO<sub>2</sub> measurements at the tower. We defined the top of the stable ABL as the height at which CO<sub>2</sub> gradients first become very small [Yi *et al.*, 2001]. The CO<sub>2</sub> mixing ratio measurements at the tower allows us to estimate the stable ABL height for very stable and moderately stable conditions as defined by Mahrt *et al.* [1998] and Mahrt [1999], but not for weakly stable conditions when the stable ABL height often exceeds 400 m.

## 2.2 Estimating the CO<sub>2</sub> Jump

The CO<sub>2</sub> jump across the nocturnal inversion was determined from the difference in CO<sub>2</sub> mixing ratios between the nocturnal ABL (geometric height weighted average values) and 396 m. Above the 200 m level, CO<sub>2</sub> mixing ratios are usually constant with time under stable conditions at night (e.g., see Figure 4 of Yi *et al.* [2001]). Therefore, the CO<sub>2</sub> mixing ratio at 396 m at night can be considered typical of the residual layer. With disturbed weather conditions such as rain, snow, heavy clouds or wind, the CO<sub>2</sub> mixing ratios at all six levels are similar and the CO<sub>2</sub> jump is very small.

The CO<sub>2</sub> jump across the top of the ML can be estimated by the ML jump model [Tennekes, 1973; Yi *et al.*, 2001]:

$$\frac{d}{dt} \Delta C = \frac{\partial C}{\partial z} \frac{dz_i}{dt} - \frac{\partial C_m}{\partial t}, \quad (1)$$

$$\frac{\partial C_m}{\partial t} = \frac{1}{z_i} \left[ (\overline{cw})_s - (\overline{cw})_i \right], \quad (2)$$

$$-(\overline{cw})_i = \Delta C \frac{dz_i}{dt}, \quad (3)$$

where  $C_m$  is the ML mean mixing ratio,  $\Delta C$  is the CO<sub>2</sub> jump across the top of the ML,  $(\overline{cw})$  is eddy covariance flux of CO<sub>2</sub>, subscript s and i refer to the surface and  $z_i$ , respectively, and  $\partial C / \partial z$  is the mixing ratio gradient above the top of the ML. Three main approximations have been made in the jump model (1)-(3). First, the influence of mean vertical velocity on the entrainment of CO<sub>2</sub> into the ML is ignored. Synoptic vertical velocity is usually smaller than the entrainment velocity. We measure  $dz_i / dt$  [Yi *et al.*, 2001], which is in truth a combination of entrainment velocity and the synoptic vertical velocity. Second, advection terms in (2) are neglected. The vertical advection is negligible everywhere except at the ML top because ML mixing ratios are nearly uniform in the vertical under convective conditions. However, significant horizontal transport of CO<sub>2</sub> could result from spatial gradient in CO<sub>2</sub> driven by different regional land cover patterns. Based on the tall tower observations, Yi *et al.* [2000] found that the relative contributions of total advection to NEE

decreases with height. The monthly mean diurnal average daytime integral (from 6:00 A.M. to 6:00 P.M.) of total advection was estimated to be 2% of the daytime integral of NEE at 30 m. Thus, we ignore advection effects under well mixed conditions.

Combining (2) and (3), we get the CO<sub>2</sub> jump,

$$\Delta C = \left[ z_i \frac{\partial C_m}{\partial t} - (\overline{cw})_s \right] / \frac{dz_i}{dt}. \quad (4)$$

All terms on the right hand side of (4) are measured from the tower and the ISS. The CO<sub>2</sub> mixing ratios at 11 m on the tower are used as  $C_m$  when the ML is shallow during the morning transition period and the average mixing ratios over six levels are used for the rest of the daytime. The CO<sub>2</sub> fluxes measured at 30 m on the tower were used as  $\overline{(cw)}_s$ . We note that (4) is only valid during the period when the ML is growing and it breaks down as  $z_i$  approaches its maximum value in the afternoon ( $dz_i/dt \rightarrow 0$ ,  $\Delta C \rightarrow \infty$ ).

In the case of  $dz_i/dt \rightarrow 0$ , the solution of (1) can be simply expressed as

$$\Delta C(t) = \Delta C(t - \Delta t) - [C_m(t) - C_m(t - \Delta t)], \quad (5)$$

An increase in the ML mixing ratio leads to a decrease in the CO<sub>2</sub> jump. Thus, when the ML reaches maximum depth, the CO<sub>2</sub> jump can be extrapolated from (5) by the tower mixing ratio measurements, assuming  $dC_{\text{trop}}/dt = 0$ .

### 2.3 Direct observations of the CO<sub>2</sub> mixing ratio profile

Shortly after sunrise, the ML begins to form near the ground with a relatively uniform CO<sub>2</sub> mixing ratio profile. When the ML is below 396 m, we define the CO<sub>2</sub> jump as the difference in CO<sub>2</sub> mixing ratio between the ML and 396 m (e. g., see Figure 4 in *Yi et al.* [2001]). As seen from Figure 1, the CO<sub>2</sub> jump calculated by the jump model during the morning hours is in good agreement with the direct observations from the tower.

The CO<sub>2</sub> Budget and Rectification Airborne study (COBRA) measured vertical profiles of CO<sub>2</sub>, H<sub>2</sub>O and potential temperature near the tower (Figure 2), thus providing a direct measurement of the CO<sub>2</sub> jump. The radar  $z_i$  measurements were consistent with the aircraft measurements in which the ML was defined to be a layer with nearly constant potential temperature (Figure 2b, 2d, 2f and 2h). The FT CO<sub>2</sub> values estimated by the jump model are in very good agreement with the aircraft measurements (Figure 2). However, additional aircraft profiling suggests that the ability of the jump model (1)-(5) to project the surface measurements to the FT is limited and is discussed later in this section.

Although only few hours were available to compare between the jump model and aircraft vertical profiles, the horizontal variability of the ML vertical profiles was clearly demonstrated by the aircraft measurements (Figure 2). These comparisons help in understanding the representativeness of the CO<sub>2</sub> jump estimated from the radar and tower measurements. Although in the ML, CO<sub>2</sub> is nearly constant with height, it varies horizontally as seen in Legs 1-3 in Figure 2c and Legs 8-9 in Figure 2a. Legs 3 and 9 may have higher ML CO<sub>2</sub> because they were near the shore of Lake

Superior (Table 1) where there is little photosynthesis. Thus the CO<sub>2</sub> jumps computed at the WLEF tower may be influenced by local NEE of CO<sub>2</sub>. The aircraft data (Figure 2) also indicate, as expected from previous studies of ABL structure, that the interface between the ML and FT is much more complicated than the simple step function assumed by the jump model (*Lily, 1968; Tennekes, 1973; Mahrt and Lenschow, 1976; Deardorff, 1979*).

To further test the ability of the jump model and tower observations to determine the FT CO<sub>2</sub> mixing ratio, we compare our tower-based estimates to periodic aircraft profiling campaigns, mountain-top flask observations, and marine ABL flask observations (Table 2). It is evident that the amplitude of the seasonal CO<sub>2</sub> cycle in the FT estimated from the jump model is much larger than the observed upper tropospheric seasonal amplitude. This appears to contradict the good agreement found between the morning profiles (Figure 1) and COBRA profiles (Figure 2). We hypothesize that the jump model calculation gives an indication of the CO<sub>2</sub> mixing ratio in FT air that is in direct contact with the ML (e.g. the upper reaches of the ABL entrainment zone). The aircraft profiles support our assertion that the CO<sub>2</sub> jumps estimated by the jump model represent the differences between the ML and the lower FT (Figure 3). This is the reason why the seasonal variability of FT CO<sub>2</sub> estimated by the jump model and predicted by GCM with SiB2 is much larger than the direct measurements of the FT CO<sub>2</sub> mixing ratios (Table 2). The entrainment zone can be fairly deep [*Kiemle et al, 1997; Davis et al, 1997*], but the FT can still exhibit considerable vertical structure above the ABL (Figure 3). As a result, jump model estimates of CO<sub>2</sub> in the FT are not always representative of the entire FT column. In fair weather conditions when the FT CO<sub>2</sub> mixing ratio appears fairly uniform subsidence compresses the troposphere (e.g. COBRA flights over Wisconsin), the jump model estimates appear to capture the FT CO<sub>2</sub> mean mixing ratios fairly

well. We proceed retaining all jump model FT CO<sub>2</sub> estimates and comparing these to the model-derived CO<sub>2</sub> mixing ratios in the lowest model layer above the ABL.

### 3. Results and Discussions

We present comparisons between observations at WLEF and modeled fields, focusing on surface fluxes, ABL depths, and the jump in CO<sub>2</sub> between the ML and the lowest portion of the FT (as discussed above). The comparison is divided into the diurnal and seasonal averages in an effort to differentiate the temporal scales that drive the rectifier effect.

#### 3.1 Diurnal Covariance

The nocturnal CO<sub>2</sub> jump reaches a maximum magnitude in the early morning (Figure 4) because CO<sub>2</sub> from respiration accumulates in a shallow, stable ABL with weak mixing during the night. When the turbulent ML begins to develop after sunrise, the CO<sub>2</sub> mixing ratio decreases rapidly due to turbulent mixing, the entrainment of lower-CO<sub>2</sub> air from the above, photosynthesis, and possibly by advection [Yi *et al.*, 2000]. Solar radiation is the driving force for both photosynthesis and turbulent convection. At the time of the diurnal maximum of the ABL depth in the growing season (typically 1800-2000 m), the ML CO<sub>2</sub> mixing ratio is on average 1-6 ppm lower than aloft on average (Figure 4c-f).

We compare our observations to the Colorado State University (CSU) General Circulation Model (GCM) coupled with the Simple Biosphere Model (SiB2) [Denning *et al.*, 1996a,b], which

has a strong rectifier signal [Denning *et al.*, 1999]. For all months, the ML depths calculated by the GCM are less than we observe (Figure 4), and the GCM stable ABL depths are less than or equal to the observations. Underestimates of mixing depths and flux magnitudes have opposing effects on the CO<sub>2</sub> jump across the ABL top. The observed nocturnal CO<sub>2</sub> jump exceeds that of the model (Figure 4) with a maximum discrepancy of about 18 ppm in July. At midday during the growing season the jump model estimates the jump in CO<sub>2</sub> mixing ratio across the ABL top to be, on average, 1-6 ppm, while in the GCM with SiB2 it is 1-3 ppm (Figure 4c-f). Thus, the GCM with SiB2 underestimates the diurnal covariance. Assuming that part of this jump persists as air is advected to the marine boundary layer, it is therefore likely that the coupled global model underpredicts the diurnal rectifier effect at the flask observing stations.

### 3.2 Seasonal Covariance

Seasonal covariance plays a more important role in the rectifier effect than the diurnal covariance, because seasonal changes are coherent and persistent across latitude zones [Denning *et al.*, 1996b]. To examine the seasonal covariance, we focus on the maximum daily ABL depth (afternoon) and daily integrated surface fluxes. The day-to-day evolution of the afternoon ABL CO<sub>2</sub> mixing ratio reflects in part the daily integral of the surface fluxes. Rather than comparing the day-night mixing, flux and mixing ratio differences, we contrast the daily mean properties in the dormant season versus the growing season. Strong seasonal covariance would be characterized by shallow mixing and large respiration fluxes in dormant season, and by deep mixing and large net photosynthetic fluxes in growing season. The observed seasonal distributions of maximum ABL depth, daily sum of CO<sub>2</sub> flux and CO<sub>2</sub> jump are shown in Figure 5. The winter (December through

February) ABL depth was shallowest (Figure 5a), but the largest CO<sub>2</sub> flux occurred in autumn (September through November) rather than in winter (Figure 5b).

The simulated and observed net daily CO<sub>2</sub> fluxes are very similar (Figure 5b). Compared to WLEF observations, the simulated CO<sub>2</sub> fluxes were more positive in autumn and more negative in summer. Ecosystem respiration in SiB2 is parameterized according to soil temperature and moisture, and scaled to produce perfect carbon balance (NEE=0) in the annual mean [Denning *et al.*, 1996a]. The simulated maximum ABL depths were too shallow throughout the year (Figure 5a). Under-simulated ABL depth should enhance the magnitude of the modeled CO<sub>2</sub> difference between the ABL and FT. In fact, the modeled CO<sub>2</sub> jump shows a persistent seasonal bias as compared to our tower-based estimate (Figure 5c). The winter difference between model and observations, therefore, is consistent with the forcing variables. That is, similar fluxes but shallower modeled mixing yields a larger magnitude CO<sub>2</sub> jump across the ABL top. The summer results for the CO<sub>2</sub> jump, however, contradict the shallower modeled ABL depths. This may be related to an imperfect match between the observations and model output. Our observations do not include days with cloud convection which is common during the summer months and is an important mechanism for redistributing CO<sub>2</sub> in the atmosphere [Hurwitz *et al.*, 2003].

Part of the discrepancy between the simulated and observed ABL thickness results from the definition of the ABL top in the GCM. The depth of the ABL is a prognostic variable in the model, which maintains the ABL top as a coordinate surface in order to resolve the jump in thermodynamic properties there [Suarez *et al.*, 1983; Randall *et al.*, 1992; Denning *et al.*, 1996b]. When the ABL becomes very deep, the model sacrifices vertical resolution near the surface to

maintain the ability to resolve the jump. As a compromise to avoid this problem, the bulk mixed layer in the simulations reviewed here was restricted to be no deeper than  $0.2 * (p_s - 100 \text{ mb})$  ( $p_s$  = surface pressure), which is generally about 1500 m, depending on temperature. In such situations, buoyancy and shear forcing in the ABL produce dry convective mixing with the layer above. A larger mass of air is in contact with the surface, which might correspond with the "real" ABL, but the coordinate surface at the simulated ABL is capped.

The comparison between model and observation presented here is imperfect, and this introduces uncertainty in our conclusions. First, our observations are biased towards fair weather observing conditions. Due to periods of poor observing conditions (rain, heavy cloud cover) and instrument failures, the measurements are available for only 40% of the deployed period of ISS. Under disturbed weather conditions, the ABL may not be well defined, and we are often unable to identify the ML top using the radar or the stable ABL depth using the tower CO<sub>2</sub> profile. In the GCM, the top of the ABL is a model coordinate surface and is always defined. Also, the sonic anemometers used for CO<sub>2</sub> flux measurements do not operate well during rain.

Second, our observations are a point measurement, while the results of the GCM with SiB2 represent a grid-box ( $4^\circ \times 5^\circ$ ) average value. The comparison of observed and modeled ABL depths are not likely to suffer much from this mismatch of spatial scale, but the GCM grid box is much larger than the footprint of the tower CO<sub>2</sub> flux data [Yi *et al.*, 2000; Davis *et al.*, 2003].

#### **4. Concluding Remarks**

Ecosystem CO<sub>2</sub> exchange and ABL mixing are correlated diurnally and seasonally. Tracer transport models predict that these covariance signals produce a meridional gradient of annual mean CO<sub>2</sub> concentration in the MBL that is half as strong as the signal produced by fossil fuel emissions [Denning *et al.*, 1995, 1996b]. The effect of this covariance on MBL CO<sub>2</sub> mixing ratios has been identified as the CO<sub>2</sub> rectifier effect. It has been predicted by many inversion models [Denning *et al.*, 1995; 1996b; Law and Simmonds, 1996a; Law and Rayner, 1999; Bousquet *et al.*, 2000; Gurney *et al.*, 2002, 2003]. However, observations to constrain the strength of these covariance signals in nature are lacking. We examined the strengths of these covariance signals in nature by using the measurements from the eddy flux tower, boundary layer profiling radar, aircraft, and compared the observations to that simulated by the CSU GCM with SiB2 [Denning *et al.*, 1996a,b] at WLEF. We conclude that (1) the observed diurnal and seasonal covariance between ecosystem CO<sub>2</sub> fluxes and ABL turbulent mixing are strong; (2) the global coupled model underestimates the diurnal covariance; and (3) the global model likely overestimates the seasonal covariance. However, these results are subject to significant uncertainties associated with the use of a point measurement to represent an area, and a fair weather bias in the data. More extensive observations of ecosystem fluxes and atmospheric mixing are needed for future study.

**Acknowledgments** This work was supported in part by the Department of Energy under grant number DOE/DE-FG02-97ER62457, a contribution to the joint program on Terrestrial Ecology and Global Change. NCAR's Atmospheric Technology Division managed the field deployment and operation of the NCAR Integrated Sounding System. Financial support for the ISS came from NCAR/ATD's instrument deployment pool. Work at the WLEF tower is supported by in part by the Atmospheric Chemistry Project of the Climate and Global Change Program of the National

Oceanic and Atmospheric Administration and by the Department of Energy's National Institutes for Global Environmental Change regional center at Indiana University. Also acknowledge CSU NIGEC funding. Weekly field support of the ISS was provided by the USDA Forest Service Forest Sciences Laboratory in Rhinelander, Wisconsin, courtesy of Jud Isebrands and Ron Teclaw. Bruce Cook (U. Minnesota) provided additional field support. We thank Steven Wofsy (Harvard U.) for his comments on a draft of this paper, Ron Teclaw (USDA-FS) and Conglong Zhao (U. Colorado/CIRES) for their support of the WLEF tower instrumentation. We also thank the State of Wisconsin Educational Communications Board for use of the transmitter tower facilities, and R. Strand (Park Falls, WI) for invaluable assistance enabling effective work at the tower.

## REFERENCES

- Angevine, W. M., A. B. White, and S. K. Avery, Boundary-layer depth and entrainment zone characterization with a boundary-layer profiler, *Boundary-Layer Meteorol.*, 68, 375-385, 1994.
- Angevine, W. M., P. S. Bakwin, and K. J. Davis, Wind profiler and RASS measurements compared with measurements from a 450-m tall tower, *J. Atmos. Ocean. Technol.*, 15, 818-825, 1998.
- Bakwin, P. S. P.P. Tans, D.F. Hurst and C. Zhao, Measurements of carbon dioxide on very tall towers: Results of the NOAA/CMDL program, *Tellus*, 50B, 401-415, 1998.

- Baldocchi, D. D., Falge, E, Gu, L., R. Olson, D. Hollinger, S. Running, P. Anthoni, Ch. Bernhofer, K. Davis, J. Fuentes, A. Goldstein, G. Katul, B. Law, X. Lee, Y. Malhi, T. Meyers, J.W. Munger, W. Oechel, K. Pilegaard, H.P. Schmid, R. Valentini, S. Verma, T. Vesala, K. Wilson and S. Wofsy, Fluxnet: a new tool to study the temporal and spatial variability of ecosystem-scale carbon dioxide, water vapor, and energy flux densities, *Bulletin of the American Meteorological Society* 82, 2415-2434, 2001.
- Berger, B. W., K. J. Davis, C. Yi, P. S. Bakwin and C. Zhao, Long-term carbon dioxide fluxes from a very tall tower in a northern forest: Flux measurement methodology, *J. Oceanic Atmos. Technol.*, 18, 529-542, 2001.
- Bousquet, P., P. Peylin, P. Ciais, C. L. Quere, P. Friedlingstein and P. P. Tans,, Regional changes in carbon dioxide fluxes of land and oceans since 1980, *Science*, 290, 1342-1346, 2000.
- Davis, K. J., D. H. Lenschow, S. P. Oncley, C. Kiemle, G. Ehret and A. Giez, The role of entrainment in surface-atmosphere interactions over the boreal forest. *J. Geophys. Res.*, 102, 29219-29230, 1997.
- Davis, K. J., P. S. Bakwin, C. Yi, B. W. Berger, C. Zhao, R. Teclaw, and J. Isebrands, The annual cycle of net CO<sub>2</sub> and H<sub>2</sub>O exchange over a northern mixed forest as observed from a very tall tower, *Global Change Biology*, 9, 1278-1293, 2003.

Denning, A. S., I. Y. Fung and D. Randall, Latitudinal gradient of atmospheric CO<sub>2</sub> due to seasonal exchange with land biota, *Nature*, 376, 240-243, 1995.

Denning, A. S., G. J. Collatz, C. Zhang, D. A. Randall, J. A. Berry, P. J. Sellers, G. D. Collello and D. A. Dazlich, Simulations of terrestrial carbon metabolism and atmospheric CO<sub>2</sub> in a general circulation model, Part 1: Surface carbon fluxes, *Tellus*, 48B, 521-542, 1996a.

Denning, A. S., D. A. Randall, G. J. Collatz and P. J. Sellers, Simulations of terrestrial carbon metabolism and atmospheric CO<sub>2</sub> in a general circulation model, Part 2: Simulated CO<sub>2</sub> concentration, *Tellus*, 48B, 543-567, 1996b.

Denning, A. S., T. Takahashi and P. Friedlingstein, Can a strong atmospheric CO<sub>2</sub> rectifier effect be reconciled with a "reasonable" carbon budget? *Tellus*, 51B, 249-253, 1999.

Deardorff, J. W., Prediction of convective mixed-layer entrainment for realistic capping inversion structure, *J. Atmos. Sci.*, 36, 424-436, 1979.

Ecklund, W. L., D. A. Carter and B. B. Balsley, A UHF wind profiler for the boundary layer: Brief description and initial results, *J. Atmos. Oceanic Technol.*, 5, 432-441, 1988.

Gurney, K. R., et al., Towards robust regional estimates of CO<sub>2</sub> sources and sinks using atmospheric transport models, *Nature*, 415, 626-630, 2002.

Gurney, K. R., et al, TransCom3 CO<sub>2</sub> inversion intercomparison: 1. Annual mean control results and sensitivity to transport and prior flux information, *Tellus*, 55B, 555-579, 2003.

Hurwitz, M.D., D.M. Ricciuto, K.J. Davis, W. Wang, C. Yi, M.P. Butler and P.S. Bakwin, Advection of carbon dioxide in the presence of storm systems over a northern Wisconsin forest, *Journal of Atmospheric Science*, (in press).

Kiemle, C., G. Ehret, A. Giez, K. J. Davis, D. H. Lenschow and S. P. Oncley, Estimation of boundary-layer humidity fluxes and statistics from airborne DIAL, *J. Geophys. Res.*, 102, 29189-29204, 1997.

Law, R. M. and I. Simmonds, The sensitivity of deduced CO<sub>2</sub> sources and sinks to variations in transport and imposed surface concentrations, *Tellus*, 48B, 613-625, 1996a.

Law, R. M., P. J. Rayner, A. S. Denning, D. Erickson, I. Y. Fung, M. Heimann, S. C. Piper, M. Ramonet, S. Taguchi, J. A. Taylor, C. M. Trudinger, and I. G. Watterson, Variations in modelled atmospheric transport of carbon dioxide and the consequences for CO<sub>2</sub> inversions, *Global Biogeochem. Cycles*, 10, 783-796, 1996b.

Law, R. M. and P. J. Rayner, Impacts of seasonal covariance on CO<sub>2</sub> inversions, *Global Biogeochem. Cycle*, 13, 845-856, 1999.

Lily, D. K., Models of cloud-topped mixed layer under strong inversion, *Quart. J. Roy. Meteorol. Soc.*, 94, 292-309, 1968.

Mahrt, L. and D. H. Lenschow, Growth dynamics of the convectively mixed layer, *J. Atmos. Sci.*, 33, 41-51, 1976.

Mahrt, L., J. Sun, W. Blumen, T. Delany and S. Oncley, Nocturnal boundary-layer regimes, *Boundary-Layer Meteorol.*, 88, 255-278, 1998.

Mahrt, L., Stratified atmospheric boundary layers, *Boundary-Layer Meteorol.*, 90, 375-396, 1999.

Masarie, K. A. and P. P. Tans, Extension and integration of atmospheric carbon dioxide data into a globally consistent measurement record, *J. Geophys. Res.*, 100, 11593-11610, 1995.

Nakazawa, T., S. Morimoto, S. Aoki and M. Tanaka, Time and space variations of the carbon isotopic ratio of tropospheric carbon dioxide over Japan, *Tellus*, 45B, 258-274, 1993.

Ottersten, H., Atmospheric structure and radar backscattering in clear air, *Radio Sci.*, 4, 1179-1193, 1969.

Press, W.H., S.A. Teukolsky, W.T. Vetterling, and B.P. Flannery, *Numerical Recipes in C*, second edition, Cambridge University Press, Cambridge, 1992.

- Randall, D. A., Q. Shao and C.-H. Moeng, A second-order bulk boundary-layer model, *J. Atmos. Sci.*, 49, 1903-1923, 1992.
- Stull, R.B., *An Introduction to Boundary-Layer Meteorology*, Kluwer, 666 pp, 1988.
- Suarez, M. J., A. Arakawa, and D. A. Randall, Parameterization of the planetary boundary layer in the UCLA general circulation model: Formulation and results, *Mon Wea. Rev.*, 111, 2224-2243, 1983.
- Tans, P. P., I. Y. Fung and T. Takahashi, Observational constraints on the global atmospheric CO<sub>2</sub> budget, *Science*, 247, 1431-1438, 1990.
- Tennekes, H., A model for the dynamics of the inversion above a convective boundary layer, *J. Atmos. Sci.*, 30, 558-567, 1973.
- White, A. B., C. W. Fairall and D. W. Thompson, Radar observations of humidity variability in and above the marine atmospheric boundary layer, *J. Atmos. Oceanic Technol.*, 8, 639-658, 1991.
- Wofsy, S.C., M.L. Goulden, J.W. Munger, S.M. Fan, P.S. Bakwin, B.C. Daube, S.L. Bassow, and F.A. Bazzaz, Net exchange of CO<sub>2</sub> in a mid-latitude forest, *Science*, 260, 1314-1317, 1993.

Wyngaard, J. C. and M. A. LeMone, Behavior of the refractive index structure parameter in the entraining convective boundary layer, *J. Atmos. Sci.*, 37, 1573-1585, 1980.

Yi, C., K. J. Davis, B. W. Berger, P. B. Bakwin, Long-term observations of the dynamics of the continental planetary boundary layer, *J. Atmos. Sci.*, 58, 1288-1299, 2001.

Yi, C., K. J. Davis, P. B. Bakwin, B. W. Berger and L. C. Marr, The influence of advection on measurements of the net ecosystem-atmosphere exchange of CO<sub>2</sub> from a very tall tower. *J. Geophys. Res.*, 105, 9991-9999, 2000.

Yi, C., K. J. Davis, P. B. Bakwin, T. Zhou, D. D. Baldocchi, M. P. Butler, B. D. Cook, A. Desai, A. L. Dunn, E. Falge, J. W. Munger, D. M. Ricciuto, W. Wang, K. Wilson, and S. C. Wofsy, The observed responses of forest carbon exchange to climate variations from daily to annual time scale, *J. Geophys. Res.*, 2003. (In review)

**Table 1.** Summary of the aircraft data for CO<sub>2</sub> and H<sub>2</sub>O shown in Figure 2.

Leg #	Latitude	Longitude	Period	Land cover	CO <sub>2</sub> * (ppm)	H <sub>2</sub> O* (g/kg)	Distance* * (km)
Leg 1	47.3348	-92.5632	1600-1700 LST 23 August 2000	Wetland	357.1	9.55	$\Delta x_{12}=89$
Leg 2	48.0618	-93.0540	1600-1700 LST 23 August 2000	Upland	359.1	8.48	$\Delta x_{23}=187$
Leg 3	46.7277	-91.5460	1600-1700 LST 23 August 2000	Shore of lake	361.4	8.71	$\Delta x_{13}=103$
Leg 4	45.9917	-90.7665	1507-1557 LST 8 June 1999	Upland	369.0	7.73	$\Delta x_{45}=40$
Leg 5	45.9322	-90.2574	1507-1557 LST 8 June 1999	Same as WLEF	364.4	9.08	
Leg 6	45.9472	-90.2221	1500-1600 LST 23 August 2000	Same as WLEF	364.1	0.54	$\Delta x_{67}=137$
Leg 7	46.5844	-91.7488	1500-1600 LST 23 August 2000	Shore of lake	365.4	1.79	
Leg 8	45.9480	-90.2715	1500-1600 LST 23 August 2000	Same as WLEF	353.3	13.03	$\Delta x_{89}=181$
Leg 9	46.8342	-92.2407	1500-1600 LST 23 August 2000	Shore of lake	360.4	9.71	
Tower	45.9458	-90.2723	1500-1600 LST 23 August 2000	Mix of wetland	353.6	12.55	$\Delta x_{1w}=234$
			1600-1700 LST 23 August 2000	and upland	354.0	12.35	$\Delta x_{2w}=316$ $\Delta x_{3w}=131$
			1500-1600 LST 8 June 1999		361.6	5.44	$\Delta x_{4w}=39$ $\Delta x_{5w}=2$ $\Delta x_{6w}=4$ $\Delta x_{7w}=134$ $\Delta x_{8w}=0$ $\Delta x_{9w}=181$

\* Values of CO<sub>2</sub> and H<sub>2</sub>O are vertical average in the mixed layer.

\*\* Subscripts i and j in  $\Delta x_{ij}$ , refer to leg number or the tower (denoted by w). The distance is the horizontal length in km between location i and j.

**Table 2.** Comparison of seasonal variability of FT CO<sub>2</sub> estimated by the zero-order jump model driven by surface measurements to direct measurements.

Site	Year	Seasonal amplitude of FT CO <sub>2</sub> (ppm)	Comment
WLEF, WI (45.95°N)	1998	15.5	Estimated from a jump model driven by surface flux and ML profiling measurements (above the ML)
Model grid including WLEF, WI (45.95°N)	-----	12.3	Above-ML CO <sub>2</sub> predicted by the CSU GCM with SiB2 [Denning <i>et al.</i> , 1995]
Marine boundary Layer (MBL) (44.4°N)	1998	6.3	Including data from sites in both the Atlantic and Pacific Ocean basins [Masarie and Tans, 1995]
CARR, CO (40.9°N)	1993-2001	5.7	Aircraft measurements were between 4 and 8 km and data were detrended.
Niwot Ridge, CO (40.0°N)	1980-2000	5.6	A mountain site (3.5 km elevation)
Between Sendai (38°N) And Fukuoka (34 °N), Japan	1979-2001	6.0	Aircraft measurements were between 4 and 8 km and data were detrended [Nakazawa <i>et al.</i> , 1993; and personal communication].

## List of Illustrations

**Figure 1.** Hourly CO<sub>2</sub> jump between the ABL and the FT calculated by the mixed layer model vs. observed values. The data were limited to the morning period of ML growth when the ML top was below 396 m. The solid line is the 1:1 line and the dotted line is an orthogonal distance linear regression [Press *et al.*, 1992] (slope = 0.95).

**Figure 2.** CO<sub>2</sub> concentrations in the ABL measured from the tower (square) and above the ABL estimated by the jump model (triangle plotted at the ML top as estimated from the ISS). Also plotted are aircraft measurements of CO<sub>2</sub> (plus and circle), H<sub>2</sub>O (diamond) and potential temperature (period). Figures are for the afternoons of 23 August of 2000, (a)-(d), and 8 June of 1999, (e)-(h). The CO<sub>2</sub> mixing ratios and fluxes measured from the tower and the ML depths derived from 915-MHz radar SNR were used in the jump model. The information about the location and land cover type of the Legs, and distance between the Legs can be found in Table 1.

**Figure 3.** Seasonal CO<sub>2</sub> vertical profiles from aircraft measurements over north central Colorado once a week (40.9 N, -104.8 W) from 1993 through 2001. The dotted lines indicate standard deviation of the mean. These data were detrended. The seasonal amplitude of FT CO<sub>2</sub> (above 4 km) is about 5.7 ppm. Let  $\delta C_{\max} = C_{\max} - C_{\min}$ , here  $C_{\max}$  and  $C_{\min}$  are maximum and minimum CO<sub>2</sub> mixing ratios above 4 km measured for each aircraft campaign, respectively. 70% of  $\delta C_{\max}$  were within 2.3 ppm. The FT CO<sub>2</sub> is nearly constant above 4 km and has large variability below 4 km that is probably influenced by ABL mixing including clear-air convection (the ML) and shallow cumulus convection.

**Figure 4.** Monthly mean diurnal cycle of mixed layer depth (thick dashed line for observations and long dashed line for simulation [Denning *et al.*, 1996b]), stable layer depth (circle for observations and long dashed line for simulation) and CO<sub>2</sub> jump across the top of ABL (solid line with standard error for observations and without error bars for simulation) for 1998. The days represented in the observations are those for which we could identify the ABL top, and days when radar, CO<sub>2</sub> flux and mixing ratio instruments were all functioning. This represents 40% of the available days between March and October. June is absent due to missing data.

**Figure 5.** Comparison of seasonal distributions of simulated [Denning *et al.*, 1996b] (dotted lines) with observed (solid line) (a) maximum ABL depth, (b) daily integral of the surface CO<sub>2</sub> flux, and (c) CO<sub>2</sub> jump. The mixed layer depths for January, February, November and December were estimated from an empirical formula [Yi *et al.*, 2001] driven by measurements of the surface virtual potential temperature flux. Standard errors are plotted in (c) for the observations.

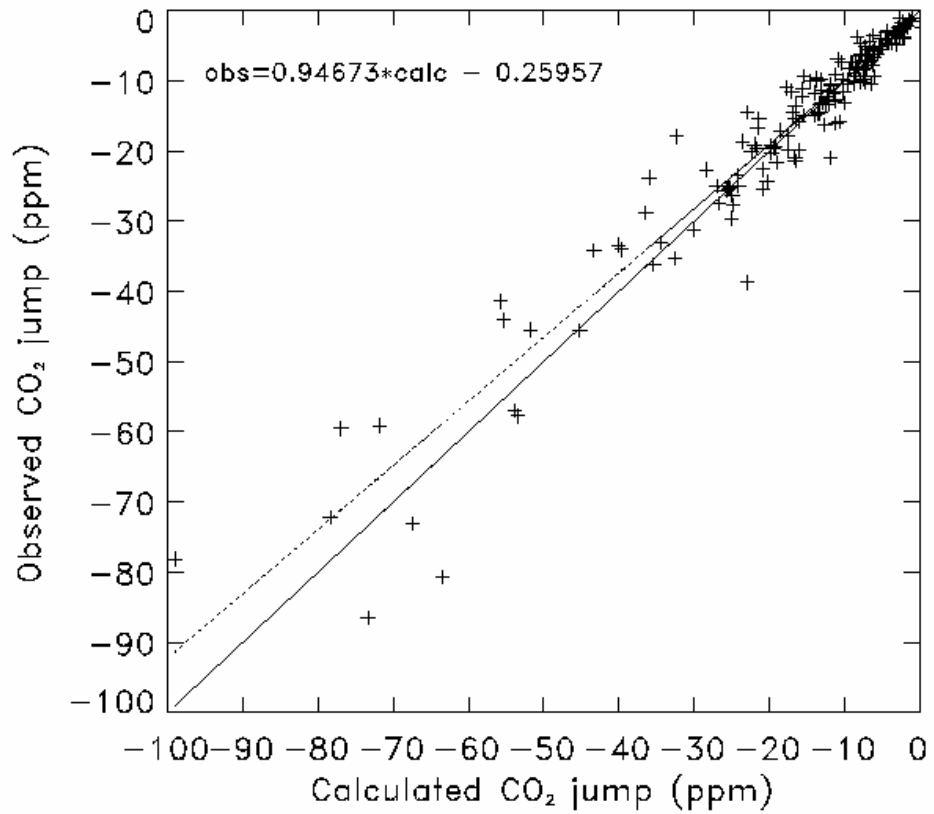


**Figure 1.** Hourly CO<sub>2</sub> jump between the ABL and the FT calculated by the mixed layer model vs. observed values. The data were limited to the morning period of ML growth when the ML top was below 396 m. The solid line is the 1:1 line and the dotted line is an orthogonal distance linear regression [*Press et al.*, 1992] (slope = 0.95).

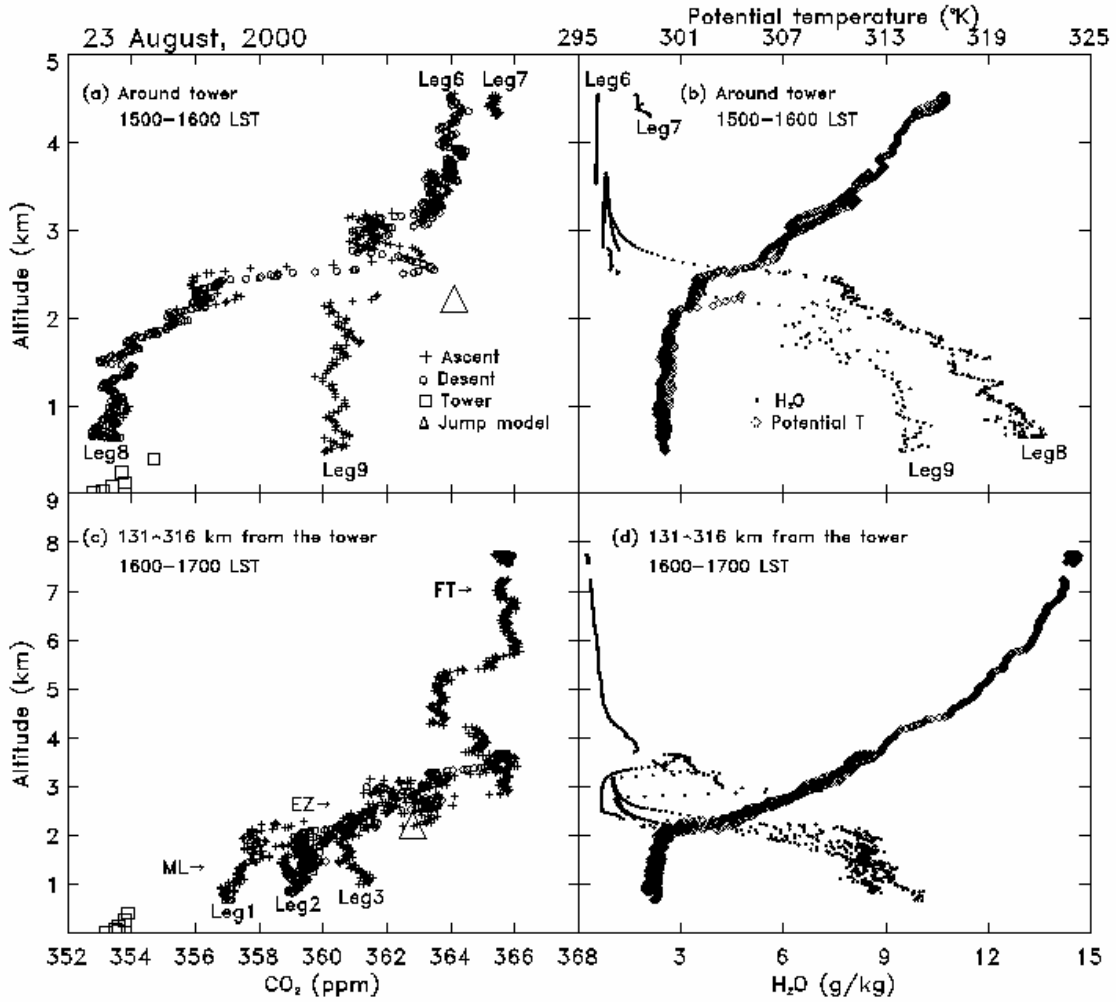


**Figure 2.** CO<sub>2</sub> concentrations in the ABL measured from the tower (square) and above the ABL estimated by the jump model (triangle plotted at the ML top as estimated from the ISS). Also plotted are aircraft measurements of CO<sub>2</sub> (plus and circle), H<sub>2</sub>O (diamond) and potential temperature (period). Figures are for the afternoons of 23 August of 2000, (a)-(d), and 8 June of 1999, (e)-(h). The CO<sub>2</sub> mixing ratios and fluxes measured from the tower and the ML depths derived from 915-MHz radar SNR were used in the jump model. The information about the location and land cover type of the Legs, and distance between the Legs can be found in Table 1.

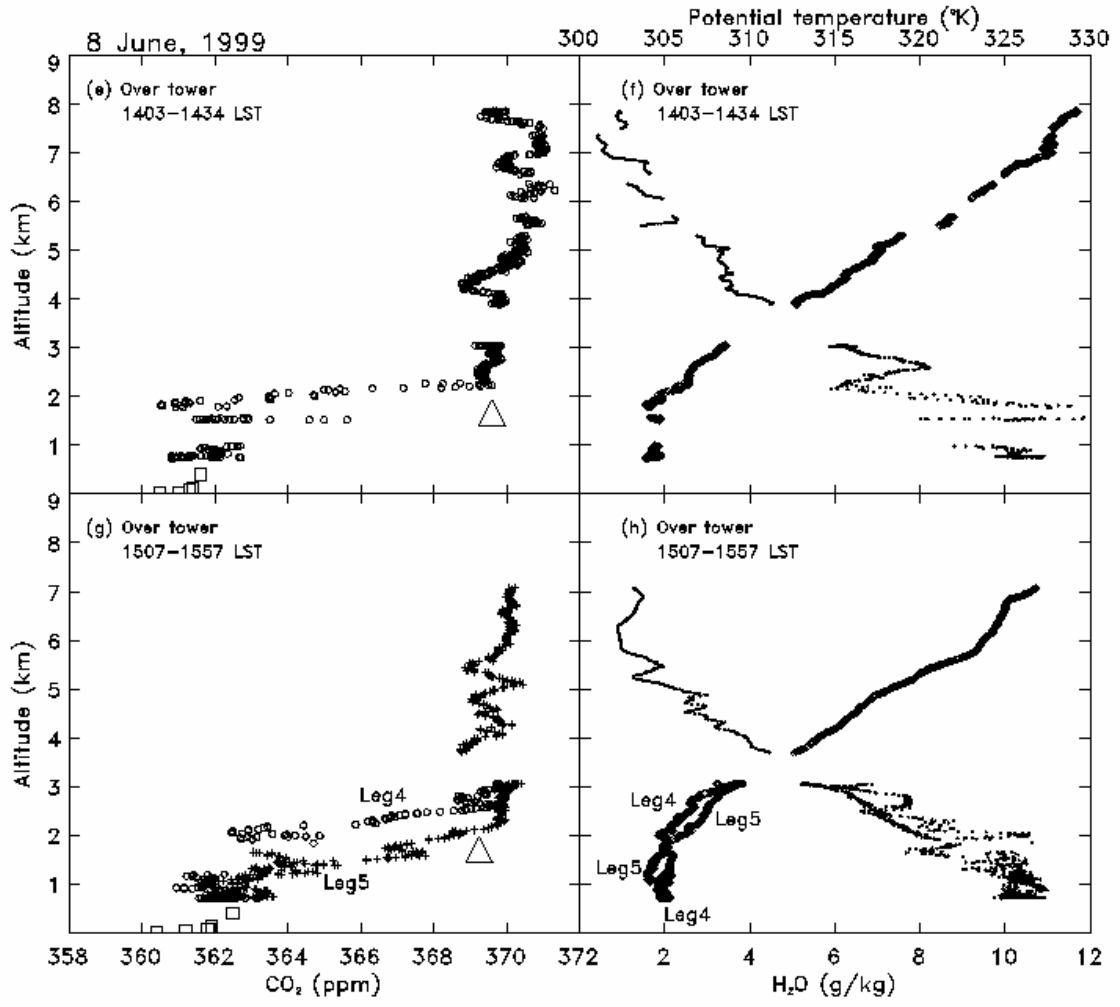
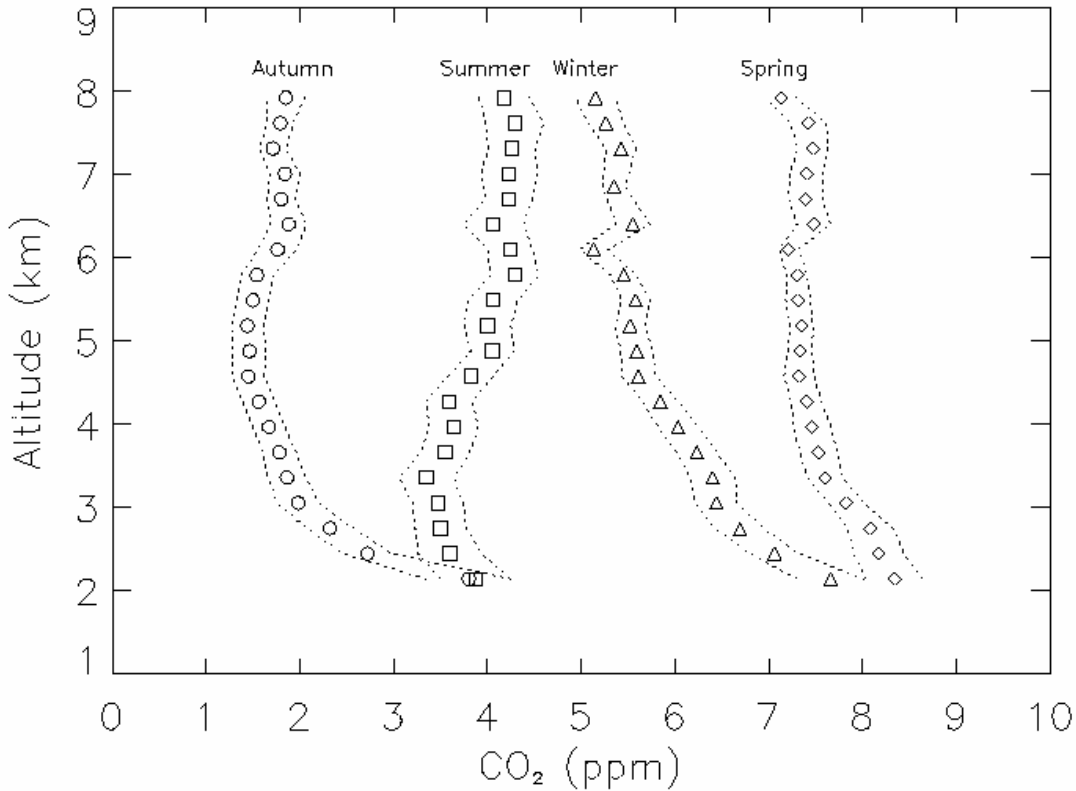
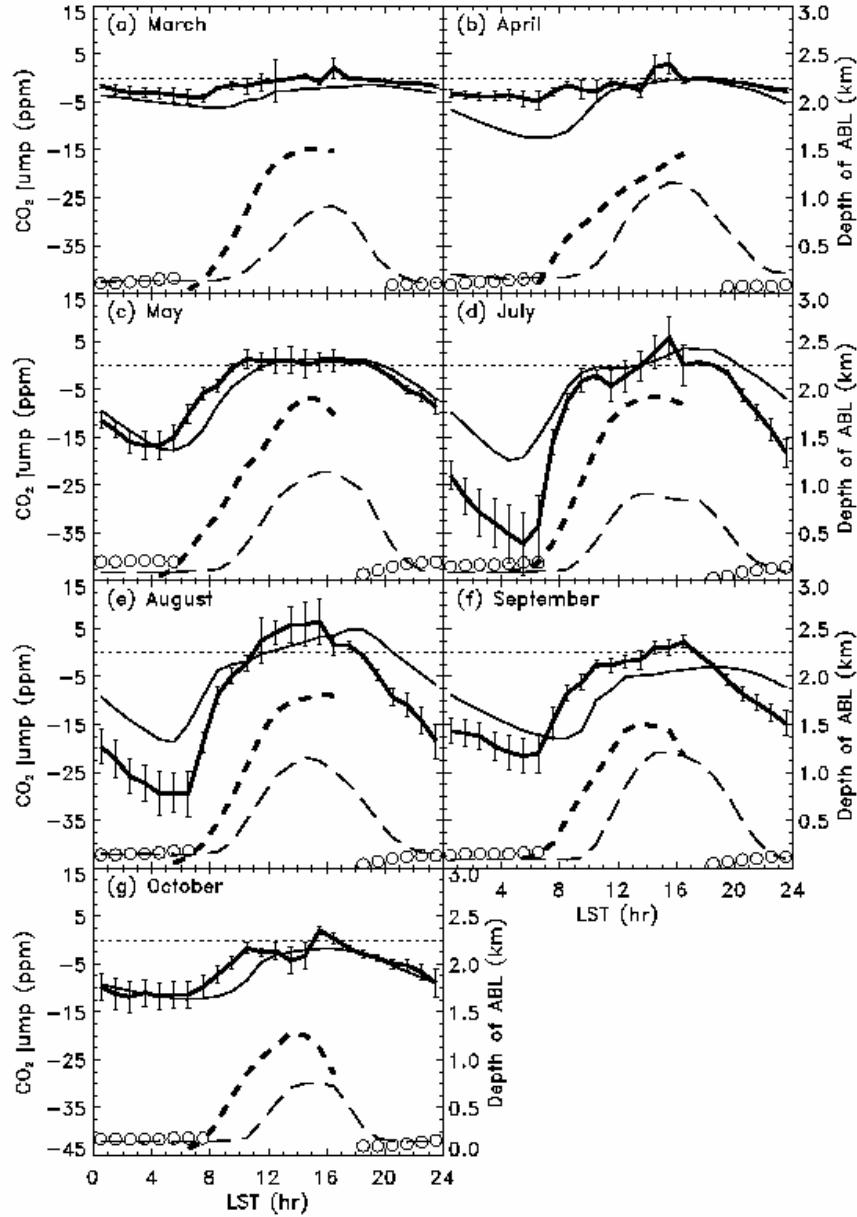


Figure 2. Continued.



**Figure 3.** Seasonal CO<sub>2</sub> vertical profiles from aircraft measurements over north central Colorado once a week (40.9 N, -104.8 W) from 1993 through 2001. The dotted lines indicate standard deviation of the mean. These data were detrended. The seasonal amplitude of FT CO<sub>2</sub> (above 4 km) is about 5.7 ppm. Let  $\delta C_{\max} = C_{\max} - C_{\min}$ , here  $C_{\max}$  and  $C_{\min}$  are maximum and minimum CO<sub>2</sub> mixing ratios above 4 km measured for each aircraft campaign, respectively. 70% of  $\delta C_{\max}$  were within 2.3 ppm. The FT CO<sub>2</sub> is nearly constant above 4 km and has large variability below 4 km that is probably influenced by ABL mixing including clear-air convection (the ML) and shallow cumulus convection.



**Figure 4.** Monthly mean diurnal cycle of mixed layer depth (thick dashed line for observations and long dashed line for simulation [Denning *et al.*, 1996b]), stable layer depth (circle for observations and long dashed line for simulation) and CO<sub>2</sub> jump across the top of ABL (solid line with standard error for observations and without error bars for simulation) for 1998. The days represented in the observations are those for which we could identify the ABL top, and days when radar, CO<sub>2</sub> flux and mixing ratio instruments were all functioning. This represents 40% of the available days between March and October, not including June, which is absent due to missing data.

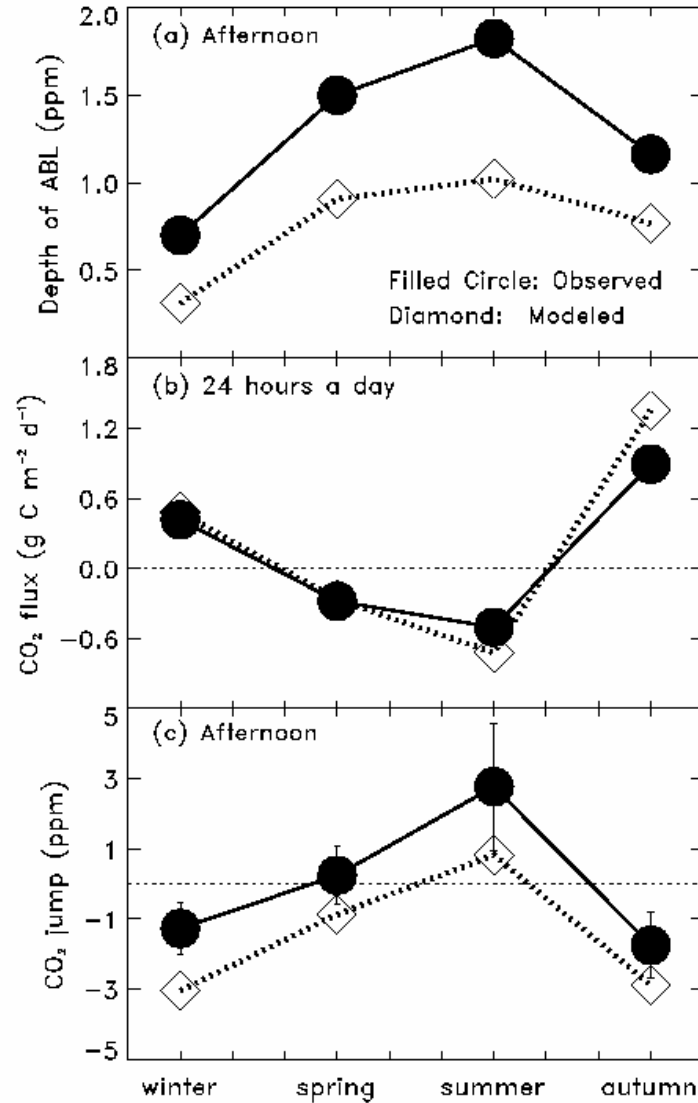


**Figure 5.** Comparison of seasonal distributions of simulated [Denning et al., 1996b] (dotted lines) with observed (solid line) (a) maximum ABL depth, (b) daily integral of the surface CO<sub>2</sub> flux, and (c) CO<sub>2</sub> jump. The mixed layer depths for January, February, November and December were estimated from an empirical formula [Yi et al., 2001] driven by measurements of the surface virtual potential temperature flux. Standard errors are plotted in (c) for the observations.